



Shahid Chamran
University of Ahvaz

Journal of Applied and Computational Mechanics



Research Paper

Inhomogeneous Gradient Poiseuille Flows of a Vertically Swirled Fluid

Natalya Burmasheva^{1,2}, Sergey Ershkov³, Evgeniy Prosviryakov^{1,2}, Dmytro Leshchenko⁴

¹ Sector of Nonlinear Vortex Hydrodynamics, Institute of Engineering Science of Ural Branch of the Russian Academy of Sciences, 34 Komsomolskaya st., Ekaterinburg, 620049, Russia, Email: nat_burm@mail.ru (N.B.); e.iu.prosviryakov@urfu.ru (E.P.)

² Academic Department of Information Technologies and Control Systems, Ural Federal University, 19 Mira st., Ekaterinburg, 620049, Russia

³ Plekhanov Russian University of Economics, Scopus number 60030998, 36 Stremyanny lane, Moscow, 117997, Russia, Email: sergej-ershkov@yandex.ru

⁴ Odessa State Academy of Civil Engineering and Architecture, Odessa, Ukraine, Email: leshchenkodmytro@gmail.com

Received June 02 2023; Revised July 10 2023; Accepted for publication July 13 2023.

Corresponding author: D. Leshchenko (leshchenkodmytro@gmail.com)

© 2023 Published by Shahid Chamran University of Ahvaz

Abstract: An exact solution is proposed for describing the steady-state and unsteady gradient Poiseuille shear flow of a viscous incompressible fluid in a horizontal infinite layer. This exact solution is described by a polynomial of degree N with respect to the variable y where the coefficients of the polynomial depend on the coordinate z and time t , a boundary value problem for a steady flow has been considered and the velocity field with a quadratic dependence on the horizontal longitudinal (horizontal) coordinate y is considered. The coefficients of the quadratic form depend on the transverse (vertical) coordinate z . Pressure is a linear form of the horizontal coordinates x and y . The exact solution of the constitutive system of equations for the boundary value problem is considered here to be polynomial. The boundary value problem is solved for a non-uniform distribution of velocities on the upper non-deformable boundary of an infinite horizontal liquid layer. The no-slip condition is set on the lower non-deformable boundary. The exact solution obtained is a polynomial of the tenth degree in the coordinates x , y and z . Stratification conditions are obtained for the velocity field, for the stress tensor components, and for the vorticity vector. The constructed exact solution describes the counterflows of a vertically swirling fluid outside the field of the Coriolis force. Shear stresses are tensile and compressive relative to the vertical (transverse) coordinates and relative to the horizontal (longitudinal) coordinates. The article presents formulas illustrating the existence of zones of differently directed vortices.

Keywords: Exact solution, overdetermined system, Poiseuille flow, vertically swirling fluid, countercurrents, stratification, reduced symmetry, Hopf bifurcation.

1. Introduction

Poiseuille exact solution is a fundamental result in classical hydrodynamics [1-4]. This exact solution describes the fluid flow between two boundaries under the action of a pressure gradient. Poiseuille exact solution is used to formulate problems in the theory of hydrodynamic stability [5-9]. The Poiseuille flow is important not only for theoretical studies of hydrodynamic problems, but it is also used to describe fluid flows in various processes. The Poiseuille flow is a basic tool for describing gradient flows in power engineering and micro-hydrodynamics [10-12]. It allows one to study the features of flows in various force fields and for various types of boundary conditions on the channel walls [10-12]. Poiseuille's classical exact solution turned out to be useful for constructing families of exact solutions for non-Newtonian fluids [13-16]. The superposition of the Ekman velocity field [17] and the Poiseuille pressure field [1-4] makes it possible to describe isobaric and gradient fluid flows in the World Ocean [4, 18-20]. Poiseuille's exact solution is useful in the study of micropolar fluids and fluids with pair stresses [21]. In addition, it can be used for creeping and many other gradient fluid flows [16, 22-25].

The Poiseuille flow has been studied by methods of group analysis [4, 20, 26-29]. The articles [27-33] contain results that made it possible to obtain new families of exact solutions of the Navier-Stokes equations. These families belong to Lin-Sidorov-Aristov class of exact solutions [34-36]. It is characterized by the dependence of the velocity field on two coordinates. Linear form coefficients depend on the third coordinate and time.

When constructing new classes of exact solutions, it is useful to remember that the Poiseuille [1, 2] gradient flow is described by the Couette or Stokes profile for velocity [37, 38, 4]. The Couette flow and the Stokes oscillatory motion belong to the class of gradientless (isobaric) motion of a viscous incompressible fluid. For unidirectional flows, the problem of integrating an ordinary differential equation (steady flow) and an equation of the heat conduction type (unsteady flow) is quite simple. If we consider two-dimensional motions in terms of velocities $V(x, y, t) = (V_x(x, y, t), V_y(x, y, t), 0)$, then the system of Navier-Stokes equations and the equations of continuity (incompressibility) becomes overdetermined [39-42]. This greatly complicates the study of the



construction of exact solutions. All known exact solutions for isobaric motions of a continuous medium for plane flows are given in articles and monographs [39-44]. For viscous incompressible fluids, the search for exact solutions for shear flows was started by Berker [39, 40] and completed by Shmyglevsky [41, 42].

In the papers, the first exact solutions for shear flows with two-dimensional velocity fields depending on three coordinates and time $\mathbf{V}(x, y, z, t) = (V_x(x, y, z, t), V_y(x, y, z, t), 0)$ were obtained and studied [45-47]. This exact solution $\mathbf{V}(x, y, z, t) = (U(z, t) + yu(z, t), V(z, t), 0)$ was constructed in the Lin-Sidorov-Aristov class [34-36].

The articles [4, 48, 49] were the first efforts to study the exact Poiseuille solution for a vertically swirling fluid excluding the field of Coriolis forces. This exact solution describes inhomogeneous fluid flows. It is based on the exact solution for inhomogeneous Couette-type flows. In the articles [4, 45-47] exact solutions were proposed for describing isobaric flows with a velocity field that depends nonlinearly on a part of the coordinates. This article generalizes the exact solution for isobaric flows of a viscous incompressible fluid for gradient flows [4, 50, 51]. The case of a velocity field with a quadratic dependence on the horizontal coordinate is considered in detail. The coefficients of the quadratic form for a steady flow depend on the transverse coordinate. It is shown that the velocity field has several stagnant points. In other words, the stratification of the velocity field takes place when the nonlinear effects of the boundary conditions are taken into account.

2. Class of Exact Solutions for the Navier-Stokes Equations

The following system of partial differential equations is traditionally used to describe shear gradient flows of a viscous incompressible pressure fluid [18]:

$$\frac{d\mathbf{V}}{dt} = -\nabla P + \nu \Delta \mathbf{V}; \quad (1)$$

$$\nabla \cdot \mathbf{V} = 0. \quad (2)$$

The nonlinear system (1) and (2) consists of the Navier-Stokes equation (1) and the continuity equation (2). Here, $\mathbf{V}(x, y, z, t) = (V_x, V_y, V_z) = (V_x, V_y, 0)$ is fluid velocity vector; P is the pressure taken relative to constant fluid density ρ ; ν is the kinematic viscosity of the fluid; $\nabla = \mathbf{i} \partial / \partial x + \mathbf{j} \partial / \partial y + \mathbf{k} \partial / \partial z$ is the Hamilton operator, $\Delta = \partial^2 / \partial x^2 + \partial^2 / \partial y^2 + \partial^2 / \partial z^2$ is the Laplace operator. The velocity vector $\mathbf{V}(x, y, z, t) = (V_x(x, y, z, t), V_y(x, y, z, t), 0)$ describes shear flow of a viscous incompressible fluid ($V_z = 0$). The remaining components of the velocity vector depend on three coordinates and time.

We study next the gradient Poiseuille shear flows in a rectangular Cartesian coordinate system. In this case, the system of equations (1), (2) has the following form [4, 48, 49]:

$$\begin{aligned} \frac{\partial V_x}{\partial t} + V_x \frac{\partial V_x}{\partial x} + V_y \frac{\partial V_x}{\partial y} &= -\frac{\partial P}{\partial x} + \nu \left(\frac{\partial^2 V_x}{\partial x^2} + \frac{\partial^2 V_x}{\partial y^2} + \frac{\partial^2 V_x}{\partial z^2} \right); \\ \frac{\partial V_y}{\partial t} + V_x \frac{\partial V_y}{\partial x} + V_y \frac{\partial V_y}{\partial y} &= -\frac{\partial P}{\partial y} + \nu \left(\frac{\partial^2 V_y}{\partial x^2} + \frac{\partial^2 V_y}{\partial y^2} + \frac{\partial^2 V_y}{\partial z^2} \right); \end{aligned} \quad (3)$$

$$\frac{\partial P}{\partial z} = 0;$$

$$\frac{\partial V_x}{\partial x} + \frac{\partial V_y}{\partial y} = 0. \quad (4)$$

The system of equations (3), (4) is overdetermined. The system (3), (4) consists of four equations for determining the velocities V_x , V_y , and pressure P . Obviously, the number of unknown functions is less than the number of equations. In addition, the third equation (hydrostatic condition) of system (3), (4) can be interpreted as a condition on the structure of the pressure function P .

The first nontrivial exact solutions to system (3), (4) were constructed within the Lin-Aristov-Sidorov class of solutions in works [4, 45-47]:

$$\begin{aligned} V_x &= U(z, t) + u(z, t)y; \quad V_y = V(z, t); \\ P &= P_0(t) + P_1(t)x + P_2(t)y. \end{aligned} \quad (5)$$

By the rotation transformation:

$$x \rightarrow x \cos \theta - y \sin \theta, \quad y \rightarrow x \sin \theta + y \cos \theta,$$

$$V_x \rightarrow V_x \cos \theta - V_y \sin \theta, \quad V_y \rightarrow V_x \sin \theta + V_y \cos \theta,$$

we obtain:

$$\begin{aligned} V_x &= U(z, t) \cos \theta - V(z, t) \sin \theta + xu(z, t) \cos \theta \sin \theta + yu(z, t) \cos^2 \theta; \\ V_y &= U(z, t) \sin \theta + V(z, t) \cos \theta - xu(z, t) \sin^2 \theta - yu(z, t) \cos \theta \sin \theta, \end{aligned} \quad (6)$$

$$P = P_0(t) + xP_1(t)(\cos \theta + \sin \theta) + yP_2(t)(\cos \theta - \sin \theta).$$



Here θ is an arbitrary constant and the function u satisfies the parabolic equation:

$$\frac{\partial u}{\partial t} = \nu \frac{\partial^2 u}{\partial z^2}.$$

In the rotation transformation above, an arrow is introduced to indicate the conversion between old and new variables by denoting them with the same symbols. Solution (5) is obtained by substituting the value $\theta = 0$ into expressions (6).

For the solution class (6), system of equations (3), (4) is reduced to a simpler system, inheriting the nonlinear properties of system (3). Thus, solution (5) can be generalized by writing the velocity field as:

$$\begin{aligned} V_x &= F(y, z, t); \\ V_y &= V(z, t). \end{aligned} \quad (7)$$

Exact solution (7) identically satisfies the continuity equation in (3), and the velocities V_x and V_y are calculated from the following system of parabolic equations:

$$\frac{\partial F}{\partial t} + V \frac{\partial F}{\partial y} = -\frac{\partial P}{\partial x} + \nu \left(\frac{\partial^2 F}{\partial y^2} + \frac{\partial^2 F}{\partial z^2} \right); \quad (8)$$

$$\frac{\partial V}{\partial t} = -\frac{\partial P}{\partial y} + \nu \frac{\partial^2 V}{\partial z^2}, \quad (9)$$

$$\frac{\partial P}{\partial z} = 0.$$

The system of equations (8), (9) is loosely coupled since the velocity F is computed after the integration of equation (9) for the functions V and P . From equation (9) it follows that $P = P(x, y)$. Since the functions V and F determined by expression (7) are independent of the x -coordinate, it is possible to construct arbitrarily complex polynomial solutions generalizing the linear coordinate dependence of velocities. The pressure is determined by formula (5). The velocities and pressure can be represented as follows:

$$\begin{aligned} V_x &= \sum_{n=0}^N F_n \frac{y^n}{n!} = F_0 + F_1 y + F_2 \frac{y^2}{2} + \sum_{n=3}^N F_n \frac{y^n}{n!}; \\ V_y &= V(z, t), \end{aligned} \quad (10)$$

$$P = P_0(t) + P_1(t)x + P_2(t)y.$$

The exact solution was found and published in [50]. Here, $F_i = F_i(z, t)$, ($i = \overline{0, N}$). In [51], the exact Couette-type solution for $N = 2$ in (5) was analyzed. The pressure components (10) that determine the pressure due to formula (6) are supposed to be known functions. They are uniquely determined by the boundary conditions. The use of formula (10) is due to the study of exact solutions of the Navier-Stokes equations announced in the articles [4, 45-50]. Previously, we considered a special case for the velocity field (5):

$$V_x = F_0 + F_1 y; \quad V_y = V(z, t)$$

in articles [4, 45-50]. Isobaric fluid flows have been studied in works [4, 45-47]. Articles [4, 48, 49] considered Poiseuille-type gradient flows. In this case, the pressure was described by formula (6).

3. Steady-state Flow of a Viscous Incompressible Fluid

In the case of steady-state flows, all functions in expressions (10) depend only on the vertical (transverse) coordinate z . Components (10) of the pressure field will be constants. Substituting (10) into the system of equations (3) and (4), we obtain the system:

$$\begin{aligned} V \left(F_1 + F_2 y + \sum_{n=3}^N F_n \frac{y^{n-1}}{(n-1)!} \right) &= -P_1 + \nu \left(F_2 + \sum_{n=3}^N F_n \frac{y^{n-2}}{(n-2)!} + \frac{d^2 F_0}{dz^2} + y \frac{d^2 F_1}{dz^2} + \frac{y^2}{2} \frac{d^2 F_2}{dz^2} + \sum_{n=3}^N \frac{d^2 F_n}{dz^2} \frac{y^n}{n!} \right); \\ \nu \frac{d^2 V}{dz^2} &= P_2. \end{aligned} \quad (11)$$

System (11) is reduced to a system of ordinary differential equations in view of the linear independence of the finite basis of the functions $\{1, y, y^2, \dots, y^N\}$:

$$\nu \frac{d^2 V}{dz^2} = P_2; \quad (12a)$$



$$\frac{d^2 F_N}{dz^2} = 0; \quad (12b)$$

$$\nu \frac{d^2 F_{N-1}}{dz^2} = VF_N; \quad (12c)$$

$$\nu \frac{d^2 F_n}{dz^2} = VF_{n+1} - \nu F_{n+2}, \quad n = \overline{1, N-2}; \quad (12d)$$

$$\nu \frac{d^2 F_0}{dz^2} = VF_1 - \nu F_2 + P_1. \quad (12e)$$

System (12) is integrated in a sequential manner in the order in which its equations are given. This system of ordinary differential equations admits an exact polynomial solution:

$$V = \frac{P_2}{\nu} \left(\frac{z^2}{2} + c_1 z + c_2 \right); \quad (13a)$$

$$F_N = c_3 z + c_4; \quad (13b)$$

$$\nu \frac{d^2 F_{N-1}}{dz^2} = VF_N = \frac{P_2}{\nu} \left(\frac{z^2}{2} + c_1 z + c_2 \right) (c_3 z + c_4) = \frac{P_2}{\nu} \left(\frac{c_3}{2} z^3 + \left(\frac{c_4}{2} + c_1 c_3 \right) z^2 + (c_1 c_4 + c_2 c_3) z + c_2 c_4 \right); \quad (13c)$$

$$F_{N-1} = \frac{P_2}{\nu^2} \left(\frac{c_3}{40} z^5 + \left(\frac{c_4}{2} + c_1 c_3 \right) \frac{z^4}{12} + (c_1 c_4 + c_2 c_3) \frac{z^3}{6} + \frac{c_2 c_4}{2} z^2 + c_5 z + c_6 \right); \quad (13d)$$

$$\nu \frac{d^2 F_{N-2}}{dz^2} = VF_{N-1} - \nu F_N = \frac{P_2^3}{\nu^3} \left(\frac{z^2}{2} + c_1 z + c_2 \right) \times \left(\frac{c_3}{40} z^5 + \left(\frac{c_4}{2} + c_1 c_3 \right) \frac{z^4}{12} + (c_1 c_4 + c_2 c_3) \frac{z^3}{6} + \frac{c_2 c_4}{2} z^2 + c_5 z + c_6 \right) - \nu (c_3 z + c_4). \quad (13e)$$

4. Boundary Value Problem for a Generalized Inhomogeneous Poiseuille Flow

To obtain solutions in the form (10), let us consider a boundary value problem describing the flow of a fluid in an infinitely extended horizontal layer of thickness h , assuming $N = 2$. Then system (12) has the form:

$$\frac{d^2 V}{dz^2} = P_2; \quad (14a)$$

$$\frac{d^2 F_2}{dz^2} = 0; \quad (14b)$$

$$\nu \frac{d^2 F_1}{dz^2} = VF_2; \quad (14c)$$

$$\nu \frac{d^2 F_0}{dz^2} = VF_1 - \nu F_2 + P_1. \quad (14d)$$

The study of the exact solution of a system of ordinary differential equations is necessary for its comparison with the exact solution (5) for an inhomogeneous Poiseuille flow and with the exact solution (10) for an isobaric flow [45-47]. To obtain an exact solution describing a specific flow, it is necessary to set an appropriate number of boundary conditions.

We assume that the no-slip condition is satisfied at the lower non-deformable boundary $z = 0$ [51]:

$$V_x = V_y = 0. \quad (15)$$

On the upper non-deformable boundary $z = h$, the velocity components are determined by the following expressions [51]:

$$V_x = W \cos \varphi + Ay + B \frac{y^2}{2}; \quad (16a)$$

$$V_y = W \sin \varphi. \quad (16b)$$

Here, W is the constant characterizes the background value of the velocity on the surface of the liquid layer; angle φ is the direction of this speed relative to the selected coordinate system; the constant A characterizes the background value of the spatial acceleration along the axis Ox ; the constant B determines the acceleration of the change in magnitude of the component V_x on the surface of the liquid layer in the direction of the axis Oy . The fluid flow scheme is shown in Fig. 1.



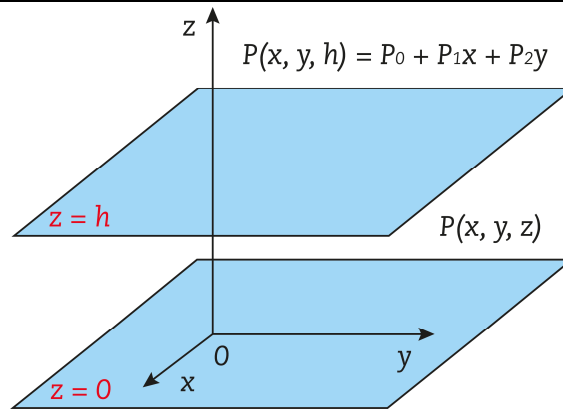


Fig. 1. Fluid flow scheme.

The coefficients (6) in the representation of the pressure field are of constant values determined by the pressure distribution, e.g., at the upper boundary.

Due to the structure of the obtained solution (11) for $N = 2$, the boundary conditions (15), (16) are reduced to the following system of constraints:

$$F_0(0) = F_1(0) = F_2(0) = 0; \quad V(0) = 0; \tag{17}$$

$$F_0(h) = W \cos \varphi; \quad F_1(h) = A; \quad F_2(h) = B; \quad V = W \sin \varphi.$$

Thus, the exact solution of the boundary value problem (14) to (16) takes the form:

$$F_0 = -\frac{Bh^2}{6}Z(-1+Z)(1+Z) + WZ \cos \varphi + \frac{Ah^2W \sin \varphi}{12\nu}(-1+Z)Z(1+Z+Z^2) + \frac{h^2P_1}{2\nu}(-1+Z)Z + \frac{Bh^4W^2 \sin^2 \varphi}{1008\nu^2}(-1+Z)Z(1+Z+Z^2)(-5+2Z^3) + \frac{Ah^4P_2}{120\nu^2}(-1+Z)Z(-2-2Z-2Z^2+3Z^3) + \frac{Bh^6W \sin \varphi P_2}{10080\nu^3}(-1+Z)Z(20+20Z+20Z^2-29Z^3-8Z^4-8Z^5+12Z^6) + \frac{Bh^8P_2^2}{201600\nu^4}(-1+Z)Z(-41-41Z-41Z^2+99Z^3+15Z^4+15Z^5-85Z^6+35Z^7); \tag{18a}$$

$$F_1 = Z \left\{ A + \frac{Bh^2W \sin \varphi}{12\nu}(-1+Z)(1+Z+Z^2) + \frac{Bh^4P_2}{120\nu^2}(-1+Z)(-2-2Z-2Z^2+3Z^3) \right\}; \tag{18b}$$

$$F_2 = BZ; \tag{18c}$$

$$V = Z \left\{ W \sin \varphi + \frac{h^2P_2}{2\nu}(-1+Z) \right\}; \tag{18d}$$

In solution (18), a replacement is introduced: $Z = z/h$ is a dimensionless vertical coordinate. This makes it possible to analyze layers of different thicknesses from the same positions.

We note that for $P_1 = P_2 = 0$, the solution (18) describes an inhomogeneous Couette flow [45-47]. If $A = B = 0$, then the velocity components have the form $V_x = W \cos \varphi Z$, $V_y = W \sin \varphi Z$, and they describe the classical layered Couette flow [4, 37], which can be reduced to a unidirectional flow by transformation of rotation [45-47]. Accounting for the quadratic term $F_2 y^2 / 2$ in the velocity field (10) leads to a more complicated exact solution of the Navier-Stokes equations. The exact solution (5) describes an inhomogeneous gradient flow of a vertically swirling fluid of the Couette-Poiseuille type. It describes the counterflow of a fluid with two stagnant points. Next, the influence of $F_2 y^2 / 2$ on the structure of the hydrodynamic flow will be shown.

5. Analysis of the Dimensionless Solution

For the convenience of further analysis of solution (18), we introduce not only the dimensionless vertical coordinate Z , but also normalize the solution as a whole by dividing the velocities by the complex Bl^2 (where l is the characteristic longitudinal or horizontal size of the layer, i.e., the characteristic scale along the Oy axis):

$$F_0 \rightarrow G_0 = \frac{F_0}{Bl^2} = -\frac{\delta^2}{6}Z(-1+Z)(1+Z) + \frac{2Re}{Ta} \cos \varphi Z + \frac{\delta^2 Re}{12a} \sin \varphi (-1+Z)Z(1+Z+Z^2) + \frac{\delta^2 \gamma_1}{2}(-1+Z)Z + \frac{\delta^4 Re^2 \sin^2 \varphi}{1008}(-1+Z)Z(1+Z+Z^2)(-5+2Z^3) + \frac{\delta^4 \gamma_2 Ta}{240}(-1+Z)Z(-2-2Z-2Z^2+3Z^3) + \frac{\delta^2 Re \gamma_2 a Ta}{20160} \sin \varphi (-1+Z)Z(20+20Z+20Z^2-29Z^3-8Z^4-8Z^5+12Z^6) + \frac{\delta^8 \gamma_2^2 a^2 Ta^2}{806400}(-1+Z)Z(-41-41Z-41Z^2+99Z^3+15Z^4+15Z^5-85Z^6+35Z^7), \tag{19a}$$



$$F_1 y \rightarrow G_1 Y = \frac{F_1 y}{Bl^2} = ZY \left\{ \frac{1}{a} + \frac{\delta^2 \text{Resin } \varphi}{12} (-1 + Z)(1 + Z + Z^2) + \frac{\delta^4 \gamma_2 a \text{Ta}}{240} (-1 + Z)(-2 - 2Z - 2Z^2 + 3Z^3) \right\}, \tag{19b}$$

$$F_2 y^2 \rightarrow G_2 Y^2 = \frac{F_2 y^2}{Bl^2} = ZY^2, \tag{19c}$$

$$V \rightarrow R = \frac{V}{Bl^2} = Z \left\{ \frac{2\text{Re}}{\text{Ta}a} \sin \varphi + \frac{\delta^2 \gamma_2}{2} (-1 + Z) \right\}. \tag{19d}$$

Here, $Z = z/h$, $Y = y/l$ are dimensionless variables; h and l are the characteristic scales in z and y respectively; $\delta = h/l$ is the parameter of the geometric anisotropy of a layer of a viscous incompressible fluid; $\text{Re} = Wl/\nu$ is Reynolds number; $\text{Ta} = 2Al^2/\nu$ is the modified Taylor number; $a = Bl/A$, $\gamma_1 = P_1/\nu B$, $\gamma_2 = P_2/\nu B$.

From the structure of the solution (19) for the function $V_y = R$, which determines the flow velocity along the Oy axis, it can be seen that this velocity takes on a zero value at the lower boundary of the layer (due to the no-slip condition) and can have one zero point inside the layer if the inequality below is satisfied:

$$\text{Resin } \varphi (4 \text{Resin } \varphi - \delta^2 \gamma_2 \text{Ta}a) < 0.$$

This velocity cannot have other zero points, since the function $V_y = R$, Eq. (19) is described by a second-order polynomial (Fig. 2). Here and below, the following values are chosen, which are used in the construction of profiles:

$$a = 9.33; \text{Ta} = 8.75; \text{Re} = -2.75; \gamma_1 = -2.35; \gamma_2 = 4.1; \delta = 0.23; \varphi = -1.5708.$$

Analyzing the properties of velocity $V_x = G_0 + G_1 Y + G_2 Y^2 / 2$ is no longer such a simple task. Among the obvious properties, one can single out the fact that this velocity takes (due to the no-slip condition) a zero value at the lower boundary of the layer, regardless of the position of the considered cross-section (the value of the Y parameter). In addition, the flow velocity along the Ox axis, due to representation (11), is determined by a nonlinear superposition of flows with velocities $G_0, G_1 Y, G_2 Y^2 / 2$. So, the base flow is the background flow with velocity G_0 . The secondary flows $G_1 Y$ and $G_2 Y^2 / 2$ (depending on the distance of the section Y) can either increase the total number of stagnant points of the resulting flow or decrease them.

We consider separately the properties of each of the three indicated flows. Let us start with something simpler. The function $G_2 Y^2$ is a strictly increasing function passing through the origin of coordinates by virtue of the presumed no-slip condition. The function $G_1 Y$ is described by the interaction of one stationary term and two monotonic terms, therefore [52] has no more than two zeros inside the considered layer.

The background component G_0 has a more complex structure, but, like the secondary fields, it is determined by the interaction of several strictly monotonic terms. Despite the fact that this is a polynomial of the ninth degree, due to [22], the number of zeros of this function belonging to the layer under consideration does not exceed six. And taking into account the rather strong relationship between the coefficients in these terms and the fact that some coefficients (e.g., $\delta^8 \gamma_2^2 a^2 \text{Ta}^2 / 806400$ or $\delta^4 \text{Re}^2 \sin^2 \varphi / 1008$) must be non-negative, the possible number of zero points within the layer is further reduced.

The velocity profiles are shown on Figs. 3 and 4 when only the background current is taken into account ($Y = 0$) and when secondary currents are taken into account ($Y = -0.003$). The velocity V_x takes on a zero value at three points. This means that the flow structure becomes more complex than the fluid flows considered in [10, 11] for an inhomogeneous flow of the Poiseuille type defined in Eq. (5).

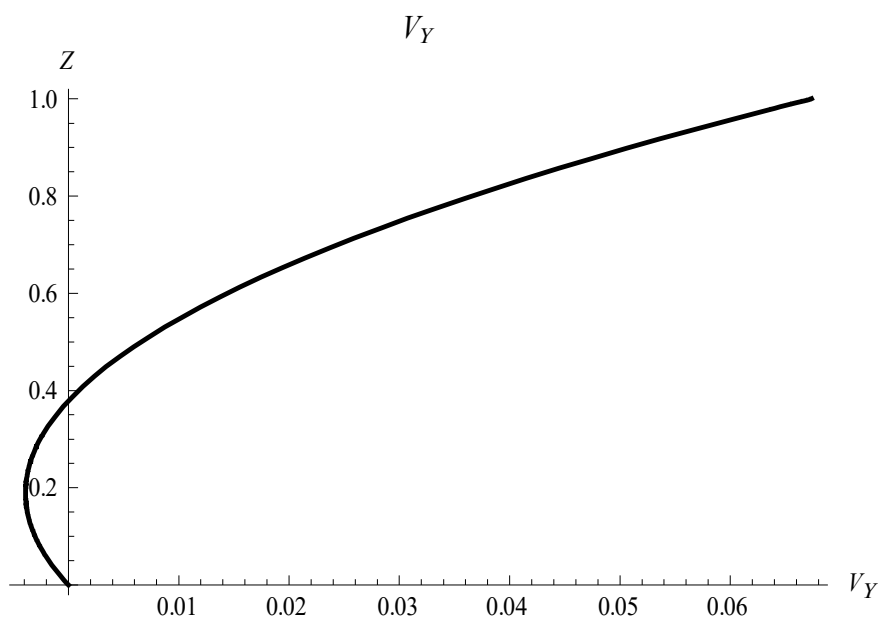


Fig. 2. Velocity Profile V_y .



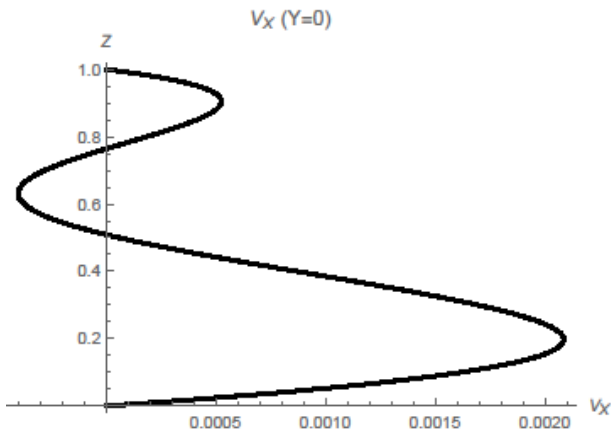


Fig. 3. Velocity profile V_x ($Y = 0$).

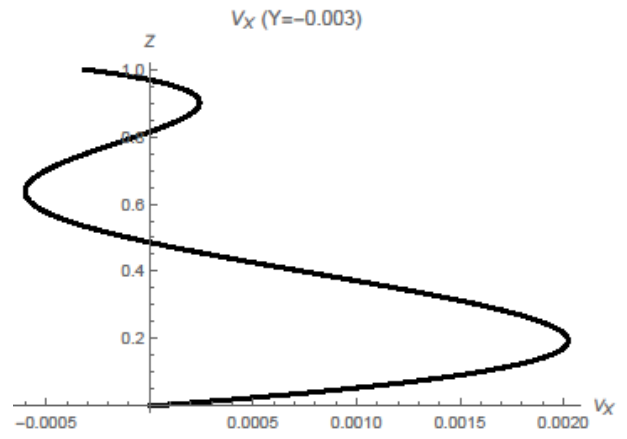


Fig. 4. Velocity profile V_x ($Y = -0.003$).

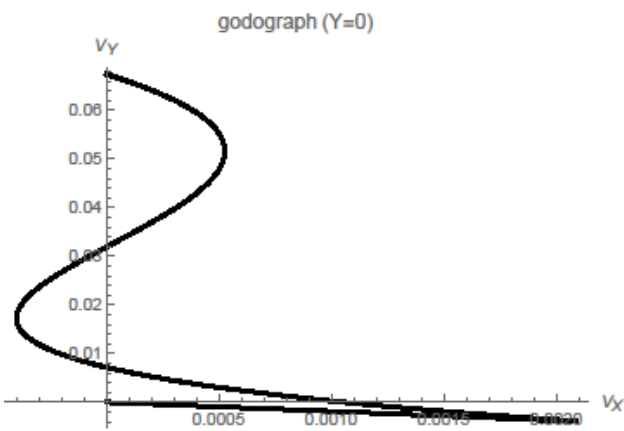


Fig. 5. Velocity vector hodograph ($Y = 0$).

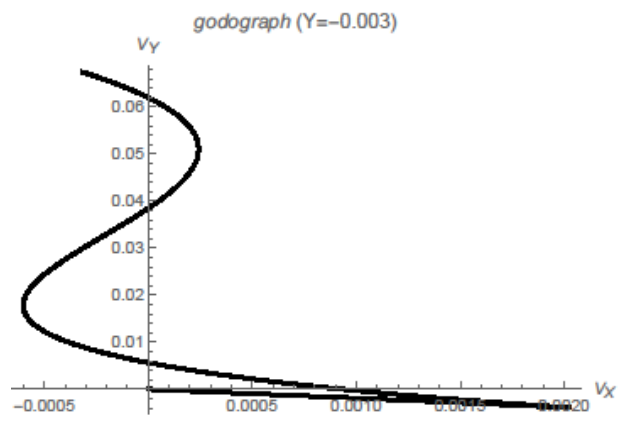


Fig. 6. Velocity vector hodograph ($Y = -0.003$).

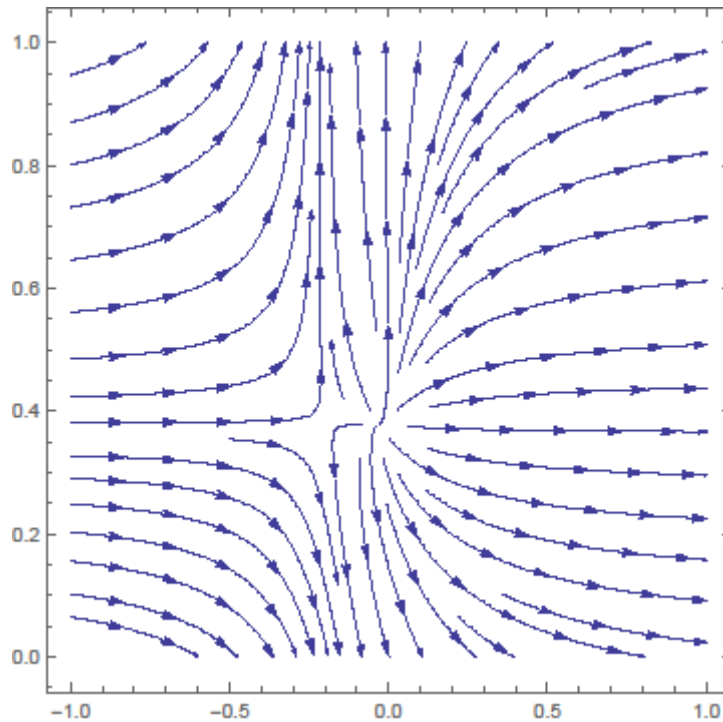


Fig. 7. Counterflows are displayed by changing the flow direction.



Figures 3 and 4 clearly illustrate that the superposition of these flows can form additional counterflow zones inside the considered layer. The hodographs of the velocity field in the two indicated sections are shown in Figs. 5 and 6. In Fig. 7, the streamlines are shown. Counterflows on the figures are displayed by changing the flow direction.

The hodographs of the velocity vector shown in Figs. 5 and 6 illustrate a spiral flow. Obviously, the vertical component of the vorticity vector $\Omega_z = \partial V_x / \partial Y$ does not equal zero. This means that there is a vertically oriented vortex in the liquid in the absence of the influence of the Coriolis force field. The stream function (Fig. 7) illustrates the effect of vertical fluid swirl on counterflows.

6. Analysis of the Vorticity Vector and Shear Stresses

Let us further consider the vorticity vector for the obtained exact solution in Eq. (19):

$$\Omega = \text{rot}\mathbf{V} = \begin{vmatrix} \mathbf{i} & \mathbf{j} & \mathbf{k} \\ \frac{\partial}{\partial x} & \frac{\partial}{\partial y} & \frac{\partial}{\partial z} \\ V_x & V_y & 0 \end{vmatrix} = -\frac{\partial V_y}{\partial z} \mathbf{i} + \frac{\partial V_x}{\partial z} \mathbf{j} + \left(\frac{\partial V_y}{\partial x} - \frac{\partial V_x}{\partial y} \right) \mathbf{k}.$$

According to the structure of solution (11) for $N = 2$, which is written in dimensionless form stemming from the form of relations (19), the dimensionless components of the vorticity vector will be determined by the following partial derivatives:

$$\Omega_x = \frac{\partial V_y}{\partial Z}; \quad \Omega_y = \frac{\partial V_x}{\partial Z}; \quad \Omega_z = \frac{\partial V_x}{\partial Y}. \tag{20}$$

We then substitute the velocity components (19) into formulas (20) and obtain the following expressions for the indicated partial derivatives:

$$\Omega_x = \frac{\partial V_y}{\partial Z} = \frac{\delta^2 \gamma_2}{2} (-1 + 2Z) + \frac{2\text{Re}}{a\text{Ta}} \sin \varphi \tag{21a}$$

$$\begin{aligned} \Omega_y = \frac{\partial V_x}{\partial Z} = & \frac{2\text{Re}}{\text{Ta}a} \cos \varphi - \frac{\delta^2}{6} (-1 + 3Z^2) + \frac{\delta^2 \text{Re}}{12a} \sin \varphi (-1 + 4Z^3) + \frac{\delta^2 \gamma_1}{2} (-1 + 2Z) + \frac{\delta^4 \text{Re}^2 \sin^2 \varphi}{1008} (5 - 28Z^3 + 14Z^6) + \\ & + \frac{\delta^4 \text{Re}^2 \sin^2 \varphi}{1008} (5 - 28Z^3 + 14Z^6) + \frac{\delta^4 \gamma_2 \text{Ta}}{240} (2 - 20Z^3 + 15Z^4) + \frac{\delta^2 \text{Re} \gamma_2 a \text{Ta}}{20160} \sin \varphi (-20 + 196Z^3 - 105Z^4 - 140Z^6 + 96Z^7) + \\ & + \frac{\delta^8 \gamma_2^2 a^2 \text{Ta}^2}{806400} (41 - 560Z^3 + 420Z^4 + 700Z^5 - 960Z^7 + 315Z^8) + Y \left\{ \frac{1}{a} + \frac{\delta^2 \text{Re} \sin \varphi}{12} (-1 + 4Z^3) + \frac{\delta^4 \gamma_2 a \text{Ta}}{240} (2 - 20Z^3 + 15Z^4) \right\} + \frac{Y^2}{2}; \end{aligned} \tag{21b}$$

$$\Omega_z = \frac{\partial V_x}{\partial Y} = \frac{Z}{120a} \{ 120 + 120aY + a^2 \gamma_2 \delta^4 \text{Ta} (2 - 5Z^3 + 3Z^4) + 10a\delta^2 \text{Re} \sin \varphi (-1 + Z^3) \} \tag{21c}$$

It follows from expressions (21) that the vortex is capable to change direction once and does not depend on the value of parameter Y (Fig. 8). The remaining two vorticity components depend on the distance of the considered section (value of parameter Y). The corresponding profiles are shown in Figs. 9 to 12.

The vortex profiles given on Figs. 8, 11, 12 show a monotonic distribution over the layer thickness. In other words, the vortex is getting stronger. This corresponds to the no-slip boundary conditions (15). The dependence of the vorticity vector component presented in Figs. 9 and 10 is nonmonotonic. This dependence illustrates the intense mixing of the liquid, taking into account other components of the vorticity vector. Assuming steady motion, one can choose the boundary conditions (16) and pressure gradients such that the fluid performs helical motions along the curvilinear axis. Stratification is observed not only for the velocity field, but also for the vorticity vector. As it will be shown below, this fact is also observed for the stress tensor components. In other words, when considering the boundary value problem (15), (16), counterflows can be detected in the liquid, accompanied by a change in the direction of rotation of the vortices. Therefore, this exact solution is suitable for designing new mixing mechanisms.

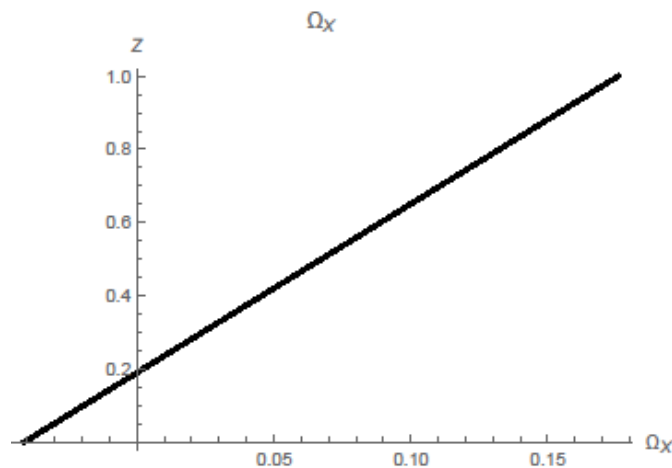


Fig. 8. Vortex profile Ω_x .



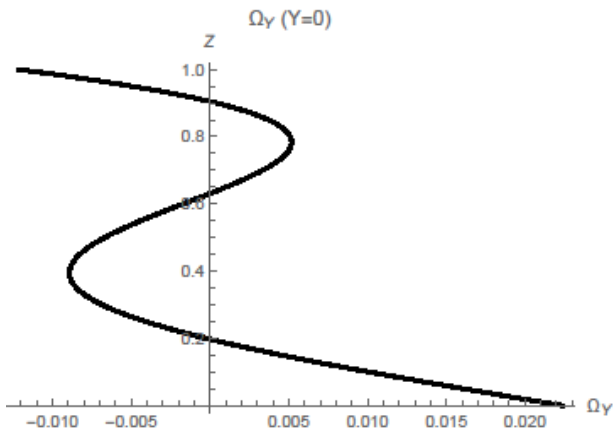


Fig. 9. Vortex profile Ω_Y (at $Y = 0$).

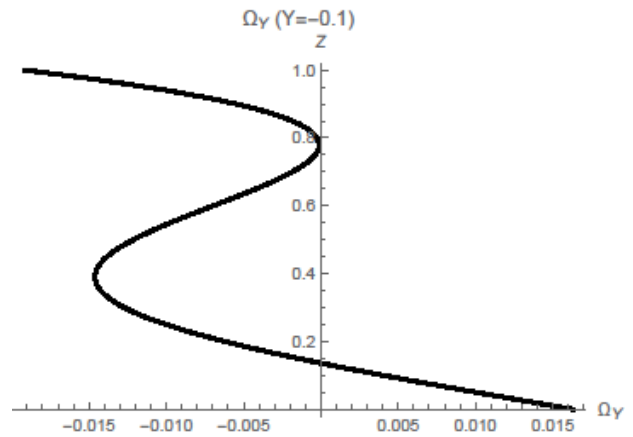


Fig. 10. Vortex profile Ω_Y ($Y = -0.1$).

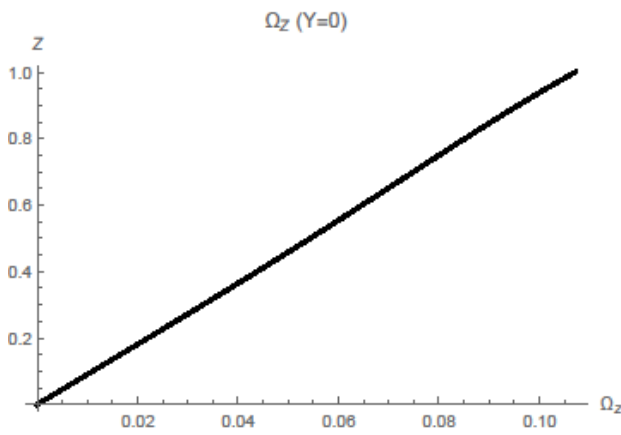


Fig. 11. Vortex profile Ω_Z ($Y = 0$).

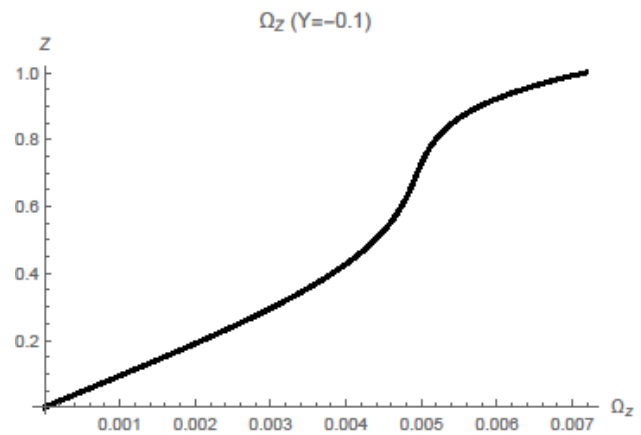


Fig. 12. Vortex profile Ω_Z ($Y = -0.1$).

At the end of our study, we should make one additional remark. It is known that the components of the stress field τ (according to the generalization of Newton's law) are determined in terms of velocities as follows:

$$\tau = \begin{pmatrix} -p + 2\eta \frac{\partial V_x}{\partial x} & \eta \left(\frac{\partial V_x}{\partial y} + \frac{\partial V_y}{\partial x} \right) & \eta \left(\frac{\partial V_x}{\partial z} + \frac{\partial V_z}{\partial x} \right) \\ \eta \left(\frac{\partial V_x}{\partial y} + \frac{\partial V_y}{\partial x} \right) & -p + 2\eta \frac{\partial V_y}{\partial y} & \eta \left(\frac{\partial V_y}{\partial z} + \frac{\partial V_z}{\partial y} \right) \\ \eta \left(\frac{\partial V_x}{\partial z} + \frac{\partial V_z}{\partial x} \right) & \eta \left(\frac{\partial V_y}{\partial z} + \frac{\partial V_z}{\partial y} \right) & -p + 2\eta \frac{\partial V_z}{\partial z} \end{pmatrix}.$$

Here p is the hydrostatic pressure, η is the dynamic viscosity coefficient of the liquid. Taking into account the structure of solution (11), we obtain simpler expressions:

$$\tau = \begin{pmatrix} -p & \eta \frac{\partial V_x}{\partial y} & \eta \frac{\partial V_x}{\partial z} \\ \eta \frac{\partial V_x}{\partial y} & -p & \eta \frac{\partial V_y}{\partial z} \\ \eta \frac{\partial V_x}{\partial z} & \eta \frac{\partial V_y}{\partial z} & -p \end{pmatrix}.$$

In other words, dimensionless shear stresses will be determined by the following partial derivatives:

$$\tau_{xy} = \eta \frac{\partial V_x}{\partial Y} = \eta \frac{\partial V_x}{\partial Y}; \quad \tau_{xz} = \eta \frac{\partial V_x}{\partial Z} = \eta \Omega_Y; \quad \tau_{yz} = \eta \frac{\partial V_y}{\partial Z} = \eta \Omega_x. \tag{22}$$

From expressions (22), it follows the nonlinear nature of the shear stresses, the qualitative behavior of which corresponds to the profiles shown in Figs. 8 to 11. In addition, the following conclusion can be drawn: some shear stresses can change sign several times in the liquid layer (they can change from tensile to compressive). In other words, the obtained solution is capable to describe not only multiple stratification of the velocity field, but also multiple stratifications of the shear stress field.



7. Results and Discussion

The exact solution (18) describes a steady inhomogeneous Couette-Poiseuille shear flow for a velocity field that is quadratically nonlinear in the y -coordinate. The coefficients of the quadratic form depend from the z -coordinate. Isobaric flow (pressure gradients are equal to zero) was studied in [51]. The exact solution (18) makes it possible to study the secondary gradient flow. If pressure gradients are taken into account, then the velocity field has an additional stratification point (stagnant point) than in isobaric flow. Exact solution (18) describes a fluid flow with vertical swirl. The vertical swirl is stratified both vertically and horizontally. The fluid performs an inhomogeneous differential spiral flow in the absence of fluid rotation (fluid motion outside the Coriolis force field). Note that there is a simple functional relationship between the components of the stress tensor and the vorticity vector. When analyzing the exact solution (18), it was found that in the case of a steady flow of fluid in each direction, zones of opposite rotation of the fluid are formed. Similarly, it can be argued that shear stresses of different signs act in a liquid. The exact solution (18) can illustrate a complex flow in the equatorial zone of the World Ocean if we use the model of shear currents with the traditional allowance for the Coriolis force (only the first Coriolis parameter is taken into account).

8. Conclusion

This paper presented the exact solution of the Navier-Stokes system of equations along with continuity equation. The study of the solution was carried out for the case of a steady gradient fluid motion. One of the longitudinal velocity components was considered to be a polynomial of degree N . For the special case $N = 2$, profiles of the obtained exact solution were constructed to illustrate the existence of counterflows in the liquid layer. The possibility of existence not less than four stagnation points in the thickness of the liquid layer was shown. In addition, the vortex structures and shear stresses that arise during the motion of the fluid were analyzed for this type of exact solution.

Finalizing conclusion section, let us remark also that useful articles regarding the exact and approximate solutions of Navier-Stokes equations should be cited [10-44], because nonstationary generalization of the aforementioned solutions of Navier-Stokes equations can be investigated as nonstationary perturbation (with given reduced symmetry or Hopf bifurcation) with respect to the invariant solutions for the problem under consideration mentioned above, at least in the vicinity of stagnation points in the thickness of the liquid layer. Stability of such solutions should be investigated in appropriate way by modern existing technique.

The exact solution obtained in the article for steady flows of the Couette-Poiseuille type can be used to study fluid motions in a horizontal layer with permeable boundaries. This exact solution can be modified to study the pressure flow in a vertical infinite layer. Obviously, it is necessary to study the hydrodynamic stability of fluid flow for the velocity field (18), which describes the Couette-Poiseuille-Nusselt flow [53].

As for explanation how the nonstationary generalization of the aforementioned solutions of Navier-Stokes equations can be investigated as nonstationary perturbation by using the concept of Hopf bifurcation (and why it can be of partial interest), let us clarify the essence of our study in regard to this matter. According to definition of Hopf bifurcation, this is the appearance or the disappearance of the periodic orbits through a local change in the stability properties of a fixed points. We can obviously and definitely state in so way insofar with respect to the invariant solutions for the problem under consideration, at least in the vicinity of stagnation points in the thickness of the liquid layer (see Fig. 7 regarding possible arising of periodic orbits in the vicinity of stagnation points).

Author Contributions

N. Burmasheva developed a technique for analyzing the exact solution and proposed a graphic design; S. Ershkov initiated the project and proposed the exact solution; E. Prosviryakov reviewed theory testing and prepared bibliographic references; D. Leshchenko checked the mathematical calculations. The manuscript was written thanks to the contribution of all authors. All authors discussed the results, reviewed and approved the final version of the manuscript.

Acknowledgments

Not applicable.

Conflict of Interest

The authors declared no potential conflicts of interest concerning the research, authorship, and publication of this article.

Funding

The authors received no financial support for the research, authorship, and publication of this article.

Data Availability Statements

The datasets generated and/or analyzed during the current study are available from the corresponding author on reasonable request.

References

- [1] Poiseuille, J.-L.-M., Recherches expérimentales sur le mouvement des liquides dans les tubes de très petits diamètres, *Comptes Rendus Hebdomadaires des Séances de l'Académie des Sciences*, 11, 1840, 961–967.
- [2] Poiseuille, J.-L.-M., Recherches expérimentales sur le mouvement des liquides dans les tubes de très petits diamètres (suite), *Comptes Rendus Hebdomadaires des Séances de l'Académie des Sciences*, 12, 1841, 112–115.
- [3] Hagen, G., Über die Bewegung des Wasser in engen cylindrischen Röhren, *Annalen der Physik*, 46, 1839, 423–442.
- [4] Ershkov, S.V., Prosviryakov, E.Y., Burmasheva, N.V., Christianto, V., Towards understanding the algorithms for solving the Navier-Stokes equations, *Fluid Dynamics Research*, 53(4), 2021, 044501.
- [5] Aristov, S.N., Gitman, I.M., Viscous flow between two moving parallel disks: exact solutions and stability analysis, *Journal of Fluid Mechanics*, 464, 2002, 209–215.
- [6] Aristov S.N., Polyaniin A.D., New Classes of Exact Solutions and Some Transformations of the Navier-Stokes Equations, *Russian Journal of*





Mathematical Physics, 17(1), 2010, 1-18.

- [7] Shalybkov, D.A., Hydrodynamic and hydromagnetic stability of the Couette flow, *Physics Uspekhi*, 52, 2009, 915–935.
- [8] Regirer, S.A., Quasi-one-dimensional theory of peristaltic flows, *Fluid Dynamics*, 19(5), 1984, 747–754.
- [9] Pedley, T.J., *The Fluid Mechanics of Large Blood Vessels. Cambridge monographs on mechanics and applied mathematics*, Cambridge University Press, 1989.
- [10] Sarkar, S., Streaming-potential-mediated pressure-driven transport of Phan-Thien–Tanner fluids in a microchannel, *Physical Review E*, 101, 2020, 053104.
- [11] Sarkar, S., Ganguly, S., Consequences of substrate wettability on the hydro-electric energy conversion in electromagnetohydrodynamic flows through microchannel, *Physica A: Statistical Mechanics and its Applications*, 542, 2020, 123450.
- [12] Roychowdhury, S., Chattopadhyay, R., Sarkar, S., Thermally developed electrokinetic bi-layer flows of Newtonian and non-Newtonian fluids in a microchannel, *Physics of Fluids*, 34(4), 2022, 042011.
- [13] Joseph, S.P., New classes of periodic and non-periodic exact solutions for Newtonian and non-Newtonian fluid flows, *International Journal of Engineering Science*, 180, 2022, 103740.
- [14] Joseph, S.P., Different families of new exact solutions for planar and nonplanar second grade fluid flows, *Chinese Journal of Physics*, 77, 2022, 1225-1235.
- [15] Hussain, E.T., Ibrahim, D.A., El-Kalaawy, O.H., Moawad, S.M., General three-dimensional equilibrium for stationary inviscid fluids in the presence of a gravitational potential, *Zeitschrift für Naturforschung A*, 78(3), 2023, 219-232.
- [16] Ershkov, S.V., Non-stationary creeping flows for incompressible 3D Navier–Stokes equations, *European Journal of Mechanics, B/Fluids*, 61(1), 2017, 154–159.
- [17] Ekman, V.W., On the Influence of the Earth's Rotation on Ocean-Currents, *Arkiv för Matematik, Astronomi och Fysik*, 2(11), 1905, 1-52.
- [18] Drazin, P.G., Riley, N., *The Navier–Stokes Equations: A classification of flows and exact solutions*, Cambridge University Press, 2006.
- [19] Aristov, S.N., Shvarts, K.G., *Vortical Flows in Thin Fluid Layers*, Vyatka State Univ. Publ., Kirov, Russian Federation, 2011 (In Russian).
- [20] Pukhnachev, V.V., Symmetries in Navier–Stokes equations, *Uspekhi Mekhaniki*, 4, 2006, 6–76 (In Russian).
- [21] Joseph, S.P., Families of superposable planar exact solutions for skew-symmetric couple stress fluid flows, *Acta Mechanica*, 2023, <https://doi.org/10.1007/s00707-023-03528-z>.
- [22] Christianto, V., Smarandache, F., An exact mapping from Navier–Stokes equation to Schrodinger equation, *Progress in Physics*, 1, 2008, 38-39.
- [23] Koterov, V.N., Shmyglevskii, Yu.D., Shcheprov, A.V., A survey of analytical studies of steady viscous incompressible flows (2000–2004), *Computational Mathematics and Mathematical Physics*, 45(5), 2005, 867-888.
- [24] Seregin, G., Šverák, V., *Regularity criteria for navier-stokes solutions*, (Book Chapter) In: Giga Y., Novotný A. (eds) *Handbook of Mathematical Analysis in Mechanics of Viscous Fluids*, Springer, Cham, 2018, 829-869.
- [25] Ershkov S.V., On Existence of General Solution of the Navier–Stokes Equations for 3D Non-Stationary Incompressible Flow, *International Journal of Fluid Mechanics Research*, 42(3), 2015, 206-213.
- [26] Shapeev, V.P., Sidorov, A.F., Yanenko, N.N., *Methods of Differential Constrains and its Applications in Gas Dynamics*, Nauka: Novosibirsk, USSR, 1984 (In Russian).
- [27] Fushchich, V.I., Popovich, R.O., Symmetry reduction and exact solutions of the Navier – Stokes equations. I., *Journal of Nonlinear Mathematical Physics*, 1, 1994, 75-113.
- [28] Fushchich, V.I., Popovich, R.O., Symmetry reduction and exact solutions of the Navier – Stokes equations. II., *Journal of Nonlinear Mathematical Physics*, 1, 1994, 156- 188.
- [29] Andreev, V.K., Kaptsov, O.V., Pukhnachev, V.V., Rodionov, A.A., *Applications of Group-Theoretical Methods in Hydrodynamics*, Springer, Dordrecht, Netherlands, 1998.
- [30] Titov, S.S., Non-local Solutions of the Cauchy Problem in Scales of Analytic Poly-algebras, *Proceedings of the Steklov Institute of Mathematics*, 9, 2003, 148-172.
- [31] Meleshko, S.V., A particular class of partially invariant solutions of the Navier–Stokes equations, *Nonlinear Dynamics*, 36, 2004, 47-68.
- [32] Fushchich, W., Popowych, R., Symmetry reduction and exact solutions of the Navier–Stokes equations, *Journal of Nonlinear Mathematical Physics*, 1, 1994, 75-98.
- [33] Ludlow, D.K., Clarkson, P.A., Bassom, A.P., Nonclassical symmetry reductions of the three-dimensional incompressible Navier–Stokes equations, *Journal of Physics A*, 31, 1998, 7965-7980.
- [34] Lin, C.C., Note on a class of exact solutions in magneto-hydrodynamics, *Archive for Rational Mechanics and Analysis*, 1, 1958, 391-395.
- [35] Sidorov, A.F., Two classes of solutions of the fluid and gas mechanics equations and their connection to traveling wave theory, *Journal of Applied Mechanics and Technical Physics*, 30(2), 1989, 197-203.
- [36] Aristov, S.N., Knyazev, D.V., Polyaniin, A.D., Exact solutions of the Navier–Stokes equations with the linear dependence of velocity components on two space variables, *Theoretical Foundations of Chemical Engineering*, 43(5), 2009, 642-662.
- [37] Couette, M., Etudes sur le frottement des liquides, *Annales de Chimie et de Physique*, 21, 1890, 433-510.
- [38] Stokes, G.G., On the effect of the internal friction of fluid on the motion of pendulums, *Transactions of the Cambridge Philosophical Society*, 9, 1851, 8-106.
- [39] Berker, R., *Sur quelques cas d'Integration des equations du mouvement d'un fluide visqueux incompressible*, Paris–Lille, Taffin–Lefort, 1936.
- [40] Berker, R., *Integration des equations du mouvement d'un fluide visqueux incompressible*, Springer–Verlag, Berlin, 1963.
- [41] Shmyglevskii, Yu.D., On Isobaric Planar Flows of a Viscous Incompressible Liquid, *Zh. Vychisl. Mat. Mat. Fiz.*, 25(12), 1985, 1895–1898 [USSR *Computational Mathematics and Mathematical Physics*, 25(6), 1985, 191–193].
- [42] Shmyglevskii, U.D., *Analytical study of the dynamics of gas and liquid*, M: Editorial URSS, 1999.
- [43] Silbergleit, A.S., Exact solution of a nonlinear system of partial differential equations arising in hydrodynamics, *Doklady Akademii Nauk*, 328, 1993, 564-566.
- [44] Ovsyannikov, L.V., Isobaric gas motions, *Diff. Uranv.*, 30(10), 1994, 1792-1799 [Differential Equations, 30(10), 1994, 1656-1662].
- [45] Aristov, S.N., Prosviryakov, E.Y., Large-scale flows of viscous incompressible vortical fluid, *Russian Aeronautics*, 58(4), 2015, 413-418.
- [46] Aristov, S.N., Prosviryakov, E.Y., Unsteady layered vortical fluid flows, *Fluid Dynamics*, 51(2), 2016, 148-154.
- [47] Prosviryakov, E.Yu., Spevak, L.F., Layered Three-Dimensional NonUniform Viscous Incompressible Flows, *Theoretical Foundations of Chemical Engineering*, 52(5), 2018, 765-770.
- [48] Burmasheva, N.V., Dyachkova, A.V., Prosviryakov, E.Yu., Inhomogeneous Poiseuille flow, *Vestnik Tomskogo Gosudarstvennogo Universiteta. Matematika i Mekhanika – Tomsk State University Journal of Mathematics and Mechanics*, 77, 2022, 68–85.
- [49] Privalova, V.V., Prosviryakov, E.Yu., Simonov, M.A., Nonlinear gradient flow of a vertical vortex fluid in a thin layer, *Russian Journal of Nonlinear Dynamics*, 15(3), 2019, 271–283.
- [50] Zubarev, N.M., Prosviryakov, E.Yu., Exact solutions for layered three-dimensional nonstationary isobaric flow of a viscous incompressible fluid, *Journal of Applied Mechanics and Technical Physics*, 60(6), 2019, 1031–1037.
- [51] Ershkov, S., Prosviryakov, E., Leshchenko, D., Exact Solutions for Isobaric Inhomogeneous Couette Flows of a Vertically Swirling Fluid, *Journal of Applied and Computational Mechanics*, 9, 2023, 521–528.
- [52] Burmasheva, N.V., Prosviryakov, E.Yu., Studying the stratification of hydrodynamic fields for laminar flows of vertically swirling fluids, *Diagnostics, Resource and Mechanics of Materials and Structures*, 4, 2020, 62–78.
- [53] Burmasheva, N., Ershkov, S., Prosviryakov, E., Leshchenko, D., Exact Solutions of Navier–Stokes Equations for Quasi-Two-Dimensional Flows with Rayleigh Friction, *Fluids*, 8, 2023, 123.


ORCID iD

Natalya Burmasheva  <https://orcid.org/0000-0003-4711-1894>

Sergey Ershkov  <https://orcid.org/0000-0002-6826-1691>

Evgeniy Prosviryakov  <https://orcid.org/0000-0002-2349-7801>



Dmytro Leshchenko  <https://orcid.org/0000-0003-2436-221X>



© 2023 Shahid Chamran University of Ahvaz, Ahvaz, Iran. This article is an open access article distributed under the terms and conditions of the Creative Commons Attribution-NonCommercial 4.0 International (CC BY-NC 4.0 license) (<http://creativecommons.org/licenses/by-nc/4.0/>).

How to cite this article: Burmasheva N., Ershkov S., Prosviryakov E., Leshchenko D. Inhomogeneous Gradient Poiseuille Flows of a Vertically Swirled Fluid, *J. Appl. Comput. Mech.*, 10(1), 2024, 1–12. <https://doi.org/10.22055/jacm.2023.43959.4150>

Publisher's Note Shahid Chamran University of Ahvaz remains neutral with regard to jurisdictional claims in published maps and institutional affiliations.

